

In summary, malonates, which are cheap and commercially available  $C_3$  building blocks, were transformed into tetra-acceptor-substituted alkenes in only two steps in excellent yields. The procedure is characterized by simple reagents, especially since only a catalytic amount of  $Mn(OAc)_3$  is required. Ultrasonication was the method of choice as it accelerates the radical reactions as well as the Knoevenagel reactions. Since radicals can be generated from various CH-acidic substrates by manganese(III), the present methodology offers promising prospects for the synthesis of other acceptor-substituted alkenes.

## Experimental Section

A solution of malonate **1** (5.0 mmol), potassium acetate (3.0 g, 31 mmol), and acetic anhydride (1.0 mL, 11 mmol) in acetic acid (40 mL) was heated to 80 °C. Manganese(III) acetate dihydrate (270 mg, 1.0 mmol) was added, and the mixture was irradiated (BANDELIN sonotrode HD200, 50 % intensity) for 3 h. After dilution with water (200 mL), the solution was extracted with dichloromethane (3 × 50 mL) and the combined organic phases were washed with a saturated sodium hydrogen carbonate solution (2 × 50 mL) and brine (50 mL). After drying (sodium sulfate) and concentration under vacuum, the unconverted malonate was removed by Kugelrohr distillation. The remaining alcohol **2** can directly be used for the next step or recrystallized from ethanol. A solution of the alcohol **2** (10.0 mmol) in dichloromethane (40 mL) was cooled to 0 °C, and triethylamine (3.0 g, 30 mmol) and a solution of methanesulfonyl chloride (2.3 g, 20 mmol) in dichloromethane (10 mL) were added dropwise at this temperature. After 2 h 10 % hydrochloric acid (50 mL) was added carefully and the combined organic phases were washed with a saturated sodium hydrogen carbonate solution (2 × 50 mL) and brine (50 mL). After drying (sodium sulfate) and concentration under vacuum the residue was crystallized from isopropanol. The alkenes **7** were isolated in analytically pure form in 98–99 % yield.

Received: June 14, 1999

Revised: November 11, 1999 [Z13553]

- [1] a) C. A. Bischoff, C. Rach, *Ber. Dtsch. Chem. Ges.* **1884**, 17, 2781–2788; b) E. Wedekind, *Ber. Dtsch. Chem. Ges.* **1901**, 34, 2077–2081; c) B. B. Corson, R. K. Hazen, J. S. Thomas, *J. Am. Chem. Soc.* **1928**, 50, 913–918.
- [2] a) D. Villemain, A. B. Alloun, *Synth. Commun.* **1992**, 22, 3169–3179; b) C. Dell'Erba, M. Novi, G. Petrillo, C. Tavani, *Tetrahedron* **1995**, 51, 3905–3914; c) J. Skarzewski, J. Zon, *Synth. Commun.* **1995**, 25, 2953–2957.
- [3] a) U. Linker, B. Kersten, T. Linker, *Tetrahedron* **1995**, 51, 9917–9926; b) T. Linker, B. Kersten, U. Linker, K. Peters, E.-M. Peters, H.-G. von Schnering, *Synlett* **1996**, 468–470; c) T. Linker, K. Hartmann, T. Sommermann, D. Scheutzw, E. Ruckdeschel, *Angew. Chem.* **1996**, 108, 1819–1821; *Angew. Chem. Int. Ed. Engl.* **1996**, 35, 1730–1732; d) T. Linker, T. Sommermann, F. Kahlenberg, *J. Am. Chem. Soc.* **1997**, 119, 9377–9384; e) T. Linker, T. Sommermann, T. Gimisis, C. Chatgililoglu, *Tetrahedron Lett.* **1998**, 39, 9637–9638; reviews of transition metal mediated radical reactions: a) J. Iqbal, B. Bhatia, N. K. Nayyar, *Chem. Rev.* **1994**, 94, 519–564; b) P. I. Dalko, *Tetrahedron* **1995**, 51, 7579–7653; c) B. B. Snider, *Chem. Rev.* **1996**, 96, 339–363; d) G. G. Melikyan, *Org. React.* **1996**, 49, 427–675; e) T. Linker, *J. Prakt. Chem.* **1997**, 339, 488–492; f) V. Nair, J. Mathew, J. Prabhakaran, *Chem. Soc. Rev.* **1997**, 127–132.
- [4] Reviews: a) R. F. Abdulla, *Aldrichimica Acta* **1988**, 21, 31–42; b) C. Einhorn, J. Einhorn, J.-L. Luche, *Synthesis* **1989**, 787–813; c) J. M. Pestman, J. B. F. N. Engberts, F. de Jong, *Recl. Trav. Chim. Pays-Bas* **1994**, 113, 533–542.
- [5] a) M. Allegretti, A. D'Annibale, C. Trogolo, *Tetrahedron* **1993**, 49, 10705–10714; b) A. D'Annibale, C. Trogolo, *Tetrahedron Lett.* **1994**, 35, 2083–2086; c) C. Bosman, A. D'Annibale, S. Resta, C. Trogolo, *Tetrahedron* **1994**, 50, 13847–13856.
- [6] J. Yamawaki, S. Sumi, T. Ando, T. Hanafusa, *Chem. Lett.* **1983**, 379–380.
- [7] J. McNulty, J. A. Steere, S. Wolf, *Tetrahedron Lett.* **1998**, 39, 8013–8016.

## Direct Evidence for Trivalent Cationic Conduction in $Nd^{3+}$ - $\beta''$ - $Al_2O_3$ \*\*

Joachim Köhler, Nobuhito Imanaka, Werner Urland, and Gin-ya Adachi\*

Dedicated to Prof. Arndt Simon  
on the occasion of his 60th birthday

The ionic conduction properties of monovalent  $M^{+}$ - $\beta''$ - $Al_2O_3$  compounds ( $M = Na, Ag, Cu$ ) have been known for decades.<sup>[1, 2]</sup> Also the migration of ions in oxides with divalent metals,  $M^{2+}$ - $\beta''$ - $Al_2O_3$  ( $M = Ca, Sr, Pb$ ), has been confirmed and identified.<sup>[3–5]</sup> On the other hand, the issue of whether or not  $M^{3+}$ - $\beta''$ - $Al_2O_3$  crystals behave as conductors with mobile  $M^{3+}$  cations as charge carriers has not yet been clarified and is still being controversially discussed. The main point of the criticism concerns the high charge of the trivalent cations. It is assumed that the resulting high Columbic interaction with the surrounding anionic host lattice prevents a corresponding current transport. Here, new experiments and results are presented for  $Nd^{3+}$ - $\beta''$ - $Al_2O_3$  crystals which directly identify and confirm the trivalent cation transport in  $M^{3+}$ - $\beta''$ - $Al_2O_3$ .

About two decades ago, the  $Na^{+}$  ions in  $Na^{+}$ - $\beta''$ - $Al_2O_3$  crystals were replaced by trivalent lanthanide cations ( $Ln^{3+}$ ).<sup>[6]</sup> The realization of these ion-exchange experiments already indicates that the trivalent cations are capable of noticeable diffusive migration at comparatively low temperatures.<sup>[7]</sup> However, the final evidence that these cations behave as charge carriers in an electric potential gradient and migrate macroscopic distances within the crystal could not be given.

Previous characterizations of  $Ln^{3+}$ - $\beta''$ - $Al_2O_3$  compounds are mainly based on impedance spectroscopy<sup>[8–11]</sup> or X-ray diffraction experiments<sup>[12–15]</sup> in which the measured impedances and electron density distributions are interpreted as the mobility of the trivalent cations. However, critics have often expressed doubt that these methods actually convey con-

[\*] Prof. G.-y. Adachi, Dr. N. Imanaka  
Department of Applied Chemistry  
Faculty of Engineering, Osaka University  
2-1 Yamadaoka, Suita, Osaka 565-0871 (Japan)  
Fax: (+81)6-6879-7352  
E-mail: adachi@chem.eng.osaka-u.ac.jp  
Dr. J. Köhler  
Department of Applied Chemistry  
Faculty of Engineering, Osaka University (Japan)  
Present address:  
Kansai Research Institute (KRI)  
Advanced Materials Research Center  
Inorganic Fine Laboratory  
Kyoto Research Park  
17 Chudoji Minami-machi, Shimogyo, Kyoto 600-8813 (Japan)  
Prof. Dr. W. Urland  
Institut für Anorganische Chemie  
Universität Hannover  
Callinstrasse 9, 30167 Hannover (Germany)

[\*\*] The fully ion exchanged  $Nd^{3+}$ - $\beta''$ - $Al_2O_3$  crystals were prepared at the Universität Hannover. The electrochemical investigations were conducted at Osaka University. J.K. gratefully acknowledges the financial support for his postdoctoral fellowship for foreign researchers in Japan by the Japan Society for the Promotion of Science (JSPS).

duction over trivalent cations. Alternative explanations for the experimental data are possible owing to a fundamental problem of ion-exchange reactions: It is impossible to achieve 100 % ion exchange of the  $\text{Na}^+$  ions by other cations. Thus, the resulting  $\text{Nd}^{3+}/\beta''\text{-Al}_2\text{O}_3$  crystals always contain, to a certain extent, remaining nonexchanged  $\text{Na}^+$  cations, which influence the conductivity measurements and which may lead to a misinterpretation of the data. Furthermore, the presence of divalent  $\text{Mg}^{2+}$  cations in the conduction planes must be assumed. Magnesium oxide is used during the synthesis of  $\text{Na}^+/\beta''\text{-Al}_2\text{O}_3$  in order to stabilize the metastable  $\beta''\text{-Al}_2\text{O}_3$  phase. The main fraction of the  $\text{MgO}$  is built into the spinel blocks of the crystal structure, but a partial incorporation of  $\text{Mg}^{2+}$  cations into the conduction planes cannot be excluded. In such a case, the  $\text{Mg}^{2+}$  cations are also assumed to be mobile and would consequently influence the electrical conductivity measurements.

Therefore, with respect to the presence of different cations within the conduction planes, experiments are needed to directly identify the migrating charge carriers. For this purpose, direct current (dc) electrolysis has turned out to be the most appropriate method. It has already been successfully used to identify the phenomenon of trivalent cationic conduction in compounds crystallizing in the  $\text{Sc}_2(\text{WO}_4)_3$  structure type.<sup>[16]</sup> In these experiments, the sample to be investigated is exposed for a given length of time to a constant potential difference, which forces the mobile cations to migrate from the anode towards the cathode. Through the use of nonreversible (ion-blocking) electrodes, characteristic cation redistributions occur at the electrodes (e.g. cation depletion at the anode, cation accumulation at the cathode), which can be measured by usual physical methods.

For the identification of trivalent cationic conduction in  $\text{M}^{3+}/\beta''\text{-Al}_2\text{O}_3$ , the choice of the appropriate electrolysis temperature is of significant importance. An interpretation of the conductivity data as a function of temperature can be found in the literature for  $\text{M}^{3+}/\beta''\text{-Al}_2\text{O}_3$  ( $\text{M} = \text{La}, \text{Nd}, \text{Pr}$ ).<sup>[15]</sup> Accordingly, the ionic conductivity at low temperatures ( $T < 250^\circ\text{C}$ ) is based only on the remaining nonexchanged  $\text{Na}^+$  cations. At higher temperatures, however, the trivalent cations also become mobile, generating a mixed cationic conduction. This transition from pure  $\text{Na}^+$  conduction to mixed  $\text{Na}^+/\text{Nd}^{3+}$  conduction occurs at about  $250^\circ\text{C}$  and can be recognized by an apparent change in the activation energies  $E_a$  ( $E_a(T > 250^\circ\text{C}) > E_a(T < 250^\circ\text{C})$ ) in the corresponding Arrhenius plots.

Following this model, two electrolysis experiments were performed below and above the transition temperature. The cation distribution patterns at the two temperatures were expected to differ significantly, and thus give rise to a clear identification of  $\text{Nd}^{3+}$  conduction. The experimental procedure for the electrolysis is schematically shown in Figure 1. Several  $\text{Nd}^{3+}/\beta''\text{-Al}_2\text{O}_3$  crystals, prepared by ion exchange of  $\text{Na}^+/\beta''\text{-Al}_2\text{O}_3$  with  $\text{NdCl}_3$ ,<sup>[17]</sup> were placed between two non-reversible (ion-blocking) platinum electrodes,<sup>[18]</sup> and a constant dc voltage was applied.<sup>[19, 20]</sup>

As shown in Figure 1c, the crystals were then cut perpendicular to the platelet plane—that is, perpendicular to the conduction planes in which the cation conduction occurs.

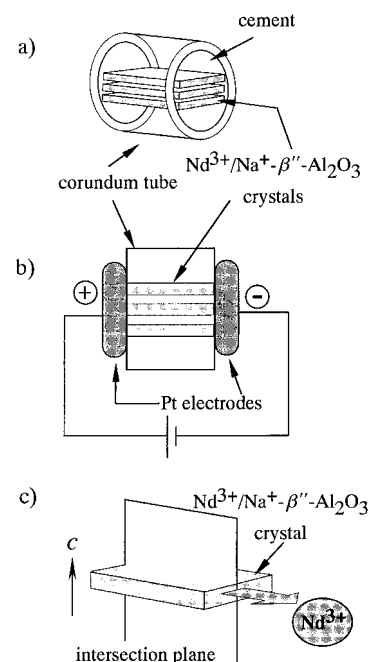


Figure 1. Schematic representation of the pellets, the electrolysis experiments, and the preparation of samples for EMPA. a) Several  $\text{Nd}^{3+}/\beta''\text{-Al}_2\text{O}_3$  crystals are fixed in a corundum tube with a cement-like binder; b) electrolysis cell containing nonreversible Pt electrodes, which are arranged perpendicular to the conduction planes of the crystals; c) intersection plane perpendicular to the conduction planes of  $\text{Nd}^{3+}/\beta''\text{-Al}_2\text{O}_3$ . The corresponding cross-section (from anode to cathode) was characterized by EPMA.

Concentration profiles of the entire cross-section of the sample were measured by electron probe microanalysis (EPMA) for the elements sodium, neodymium, aluminum, and magnesium. EPMA was also used for the characterization of the anodic and cathodic surfaces as well as for the determination of the chemical composition of the crystals before the electrolysis. The average composition of the  $\text{Nd}^{3+}/\beta''\text{-Al}_2\text{O}_3$  crystals used (averaged over ten samples) was found to be  $\text{Na}_{0.04}\text{Nd}_{0.57}\text{Mg}_{0.52}\text{Al}_{10.43}\text{O}_{17.04}$  with a degree of exchange of 97.6%.<sup>[21]</sup> Despite “complete” ion exchange, 2–3 % (based on the original sodium content) of the  $\text{Na}^+$  cations still remain within the samples.

The concentration profiles of the elements Na and Nd are shown in Figure 2 for the electrolysis of a  $\text{Nd}^{3+}/\beta''\text{-Al}_2\text{O}_3$  crystal at  $250^\circ\text{C}$ . The sodium concentration is significantly increased at the cathodic side in comparison to the uniform distribution within the bulk of the sample. The neodymium distribution is also uniform in the inner part of the crystals, whereas at the cathodic side only a comparatively slight increase can be observed. It should be noted that the concentration profile of Na, Nd, Mg, and Al for a non-electrolyzed  $\text{Nd}^{3+}/\beta''\text{-Al}_2\text{O}_3$  sample (not shown) is uniform over the whole cross-section without any significant fluctuations, even at the electrodes.

The increase in the Na content at the cathode is interpreted in terms of mobile  $\text{Na}^+$  cations that migrate toward the cathode during electrolysis. Owing to the ion-blocking properties of the platinum electrodes, the  $\text{Na}^+$  cations accumulate. On the other hand, the  $\text{Nd}^{3+}$  cations are not

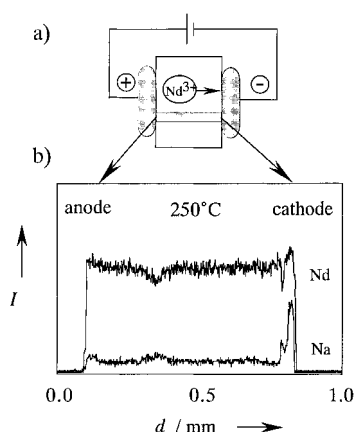


Figure 2. a) Schematic representation of the electrolysis cell; b) concentration profiles over the entire cross-section (from anode to cathode) of a  $\text{Nd}^{3+}$ - $\beta''$ - $\text{Al}_2\text{O}_3$  crystal after electrolysis at 250 °C.

sufficiently mobile at this low temperature, and a comparable increase in the Nd concentration at the cathode does not occur. It can be concluded that at temperatures below 250 °C  $\text{Na}^+$  cations represent the exclusive or main charge-carrying species.

A different result is obtained for the electrolysis of a  $\text{Nd}^{3+}$ - $\beta''$ - $\text{Al}_2\text{O}_3$  crystal at 600 °C, that is, significantly higher than the transition temperature. The measured concentration profiles for Na, Nd, and Mg are displayed in Figure 3. Like in Figure 2, a positive sodium concentration gradient appears at the cathodic side of the sample. However, in contrast to the low-temperature electrolysis, a remarkable increase in concentration can be recognized for the trivalent  $\text{Nd}^{3+}$  cation at the cathode. This differs significantly from the data of the low-temperature electrolysis. In accordance with the aforementioned model of ion conduction in  $\text{M}^{3+}$ - $\beta''$ - $\text{Al}_2\text{O}_3$ ,<sup>[15]</sup> it can be stated that the trivalent  $\text{Nd}^{3+}$  cations are mobile at higher temperatures ( $T > 250$  °C). Both  $\text{Na}^+$  and  $\text{Nd}^{3+}$  cations are forced by the potential gradient to migrate through the crystal, leading to the corresponding accumulation at the Pt cathode.

Table 1 compares the averaged data from elemental analysis (by EPMA) taken at different sites (punctual analysis) on the anodic and cathodic surfaces of a  $\text{Nd}^{3+}$ - $\beta''$ - $\text{Al}_2\text{O}_3$  sample before and after high-temperature electrolysis. In comparison to the nonelectrolyzed sample, a clear increase

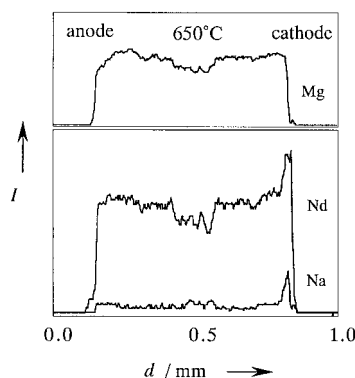


Figure 3. Concentration profiles of Na, Nd, and Mg over the entire cross-section (from anode to cathode) of a  $\text{Nd}^{3+}$ - $\beta''$ - $\text{Al}_2\text{O}_3$  crystal after electrolysis at 650 °C. The notable decrease in intensity in the middle part of the crystal is caused by a large hole in the investigated section of the sample.

Table 1. Cationic elemental analysis (EPMA) of the cathodic and anionic surfaces of a  $\text{Nd}^{3+}$ - $\beta''$ - $\text{Al}_2\text{O}_3$  sample before and after electrolysis at 650 °C. The data are given in atomic percent (at-%) and correspond to the average value of eight measurements at different sites on the sample.

Element:	Na	Nd	Mg	Al
before electrolysis (cathode and anode)	0.4	4.9	4.5	90.2
after electrolysis (cathode)	0.7	28.9	2.5	67.9
after electrolysis (anode)	0	2.3	4.8	92.9

in the Na and Nd concentration on the cathode surface and a corresponding decrease at the anodic side can be recognized.

All of the discussed observations clearly indicate the presence of mobile  $\text{Nd}^{3+}$  ions (and  $\text{Na}^+$  ions) in  $\text{Nd}^{3+}$ - $\beta''$ - $\text{Al}_2\text{O}_3$ . At the anodic side of the pellets the sample is decomposed, releasing  $\text{Nd}^{3+}$  and  $\text{Na}^+$  cations. Following the potential gradient, these cations migrate from the anode through the solid electrolyte to the cathodic side of the sample. The resulting  $\text{Nd}^{3+}$  and  $\text{Na}^+$  accumulation reflects the corresponding increase in concentration from the EPMA measurements. On the other hand, at the anodic side of the sample mainly aluminum and magnesium oxides are left.<sup>[22]</sup> Such a redistribution of, for example, neodymium would not occur if the  $\text{Nd}^{3+}$  ions are not mobile within the  $\text{Nd}^{3+}$ - $\beta''$ - $\text{Al}_2\text{O}_3$ -matrix. It is not possible to explain the results only on the basis of electrolytic decomposition and/or chemical reactions between the electrolyte and the atmosphere without assuming mobile charge carriers. Thus, these observations are the first direct and clear indication for trivalent cation conduction in  $\beta''$ - $\text{Al}_2\text{O}_3$ .

With respect to the comparatively uniform concentration profile of magnesium over the entire sample cross-section at low and high temperatures (Figure 3), it can be additionally stated that these cations are not mobile. The measurements indirectly confirm the exclusive incorporation of  $\text{Mg}^{2+}$  into the spinel blocks of the crystal structure. A comparable result could also be obtained for aluminum (the concentration profile is not shown here), indicating the nonmobility of  $\text{Al}^{3+}$ . Additional experiments, for example polarization measurements or measurements of conductivity as a function of  $\text{O}_2$  partial pressure, have been performed in order to characterize the conduction properties of  $\text{Nd}^{3+}$ - $\beta''$ - $\text{Al}_2\text{O}_3$  more thoroughly. However, the detailed description of these experiments is beyond the scope of this article and therefore not included here. It can nonetheless be stated that the electrical conduction in  $\text{Nd}^{3+}$ - $\beta''$ - $\text{Al}_2\text{O}_3$  is neither generated nor influenced by electronic or  $\text{O}^{2-}$  charge carriers.

In conclusion,  $\text{Nd}^{3+}$ - $\beta''$ - $\text{Al}_2\text{O}_3$  can be characterized as a solid electrolyte in which the electrical current is transported by mobile trivalent cations. However, the influence of the remaining nonexchanged  $\text{Na}^+$  cations, which are present in a minor concentration, on the conduction behavior cannot be neglected. The  $\text{Na}^+$  ions represent the predominant charge carriers at low temperatures, whereas at higher temperatures the  $\text{Nd}^{3+}$  ions also contribute to the current transport, generating a mixed cationic conduction. These investigations demonstrate for the first time that highly charged trivalent cations are mobile within the  $\beta''$ - $\text{Al}_2\text{O}_3$  matrix. For future studies the ambitious goal remains to quantitatively identify

the current transport by trivalent charge carriers. This challenge can be managed, for example, with “Tubandt electrolysis” experiments.

Received: July 12, 1999  
Revised: September 6, 1999 [Z13709]

- [1] Y.-F. Y. Yao, J. T. Kummer, *J. Inorg. Nucl. Chem.* **1967**, 29, 2453.
- [2] G. C. Farrington, J. L. Briant in *Fast Ion Transport in Solids* (Eds.: P. Vashista, J. N. Mundy, G. K. Shenoy), Elsevier, North-Holland, **1979**, pp. 395–400.
- [3] J. O. Thomas, M. Aldén, G. C. Farrington, *Solid State Ionics* **1983**, 9/10, 301.
- [4] R. Seevers, J. DeNuzzio, G. C. Farrington, B. Dunn, *J. Solid State Chem.* **1983**, 50, 146.
- [5] G. S. Rohrer, G. C. Farrington, *J. Solid State Chem.* **1990**, 85, 299.
- [6] B. Dunn, G. C. Farrington, *Solid State Ionics* **1983**, 9/10, 223.
- [7] The term “low temperature” is used with respect to the “normalized temperature”  $T_n < 0.5$ , with  $T_n = T_d/T_m$  ( $T_a$  is the actual operation temperature, and  $T_m$  the melting point of the compound being considered).
- [8] F. Tietz, W. Urland, *Solid State Ionics* **1995**, 78, 35.
- [9] J. Köhler, W. Urland, *Z. Anorg. Allg. Chem.* **1997**, 623, 231.
- [10] J. Köhler, W. Urland, *Solid State Ionics* **1996**, 86–88, 93.
- [11] J. Köhler, W. Urland, *J. Solid State Chem.* **1996**, 127, 161.
- [12] W. Carrillo-Cabrera, J. O. Thomas, G. C. Farrington, *Solid State Ionics* **1983**, 9/10, 245.
- [13] J. Köhler, W. Urland, *Z. Anorg. Allg. Chem.* **1996**, 622, 191.
- [14] J. Köhler, W. Urland, *J. Solid State Chem.* **1996**, 124, 169.
- [15] J. Köhler, W. Urland, *Angew. Chem.* **1997**, 109, 150; *Angew. Chem. Int. Ed.* **1997**, 36, 85.
- [16] J. Köhler, N. Imanaka, G. Adachi, *Chem. Mater.* **1998**, 10, 3790.
- [17] The  $\text{Na}^+/\beta''\text{-Al}_2\text{O}_3$  crystals were prepared by the flux–evaporation method by slowly evaporating the  $\text{Na}_2\text{O}$  flux at about 1700 °C. The ion exchange was performed by immersing the  $\text{Na}^+/\beta''\text{-Al}_2\text{O}_3$  crystals into molten anhydrous  $\text{NdCl}_3$  and heating at 760 °C for 6 d under argon. After ion exchange, the crystals have the characteristic blue-purple color of  $\text{Nd}^{3+}$  ions.
- [18] The crystals were fixed by insertion into a corundum tube and filling of the remaining spaces with a hardening liquid cement.
- [19] The applied dc voltage amounted to 6 V in both experiments. The sample was electrolyzed for 130 d in the case of the low-temperature electrolysis ( $T = 250^\circ\text{C}$ ), and for 16 d in the case of the high-temperature electrolysis ( $T = 650^\circ\text{C}$ ).
- [20] With the use of nonreversible electrodes, the applied voltage must exceed the decomposition voltage of the compound in order to generate a constant flux of charge carriers. In the case of  $\text{Nd}^{3+}/\beta''\text{-Al}_2\text{O}_3$ , the decomposition voltage was determined in advance to be about 1.5–2 V.
- [21] The degree of exchange refers to the original  $\text{Na}^+$  content of the  $\text{Na}^+/\beta''\text{-Al}_2\text{O}_3$  crystals used.
- [22] The transference numbers for the electrolysis cannot be quantitatively determined because the absolute amount of transported charge carriers is not known. The EPMA data only represent the relative cation distribution on the surface. Transported cations which are located beneath the surface are not detected.

## Extremely Strong $s^2$ – $s^2$ Closed-Shell Interactions\*\*

Ralf Wesendrup and Peter Schwerdtfeger\*

Closed-shell interactions (CSI) range from extremely weak van der Waals forces, as for the helium dimer (dissociation energy,  $E_d = 9.06 \times 10^{-2} \text{ kJ mol}^{-1}$ ),<sup>[1,2]</sup> to strong aurophilic interactions ( $E_d$  up to  $30 \text{ kJ mol}^{-1}$ ).<sup>[3]</sup> The strength of the latter lie almost in the order of covalent bonds, and strong CSI have recently been reviewed by Pyykkö.<sup>[4]</sup> The bonding situation in these compounds is described by an equal number of electrons in bonding and antibonding molecular orbitals. This gives rise to a bond order of zero and explains why CSI are generally so weak.

Unusually strong “closed-shell interactions” have recently been reported for the  $d^{10}$ – $s^2$  system  $\text{Au}^+/\text{Hg}$  ( $E_d = 179 \text{ kJ mol}^{-1}$ , Table 1),<sup>[5]</sup> and for the related cationic gold rare gas (Rg) compounds  $\text{RgAu}^+$  ( $E_d = 126 \text{ kJ mol}^{-1}$ ).<sup>[6]</sup> These

Table 1. Bond lengths  $r_e$  [Å] and dissociation energies  $E_d$  [kJ mol<sup>−1</sup>] (not corrected for zero-point vibration) at various levels of theory.

	AuM		AuM		AuM <sup>−</sup>	
	$r_e$	$E_d$	$r_e$	$E_d$	$r_e$	$E_d$
$M = \text{Hg}^{+[\text{a}]}$						
R-HF	2.700	119.4	–	–	3.293	13.4
R-MP2	2.528	197.2	2.630	56.3	2.838	58.1
R-CCSD	2.590	168.5	2.743	28.8	3.018	30.4
R-CCSD(T)	2.581	179.2	2.711	37.6	2.967	36.8
NR-HF	3.066	89.8	–	–	3.631	15.4
NR-MP2	2.794	145.9	2.883	41.7	3.016	59.3
$M = \text{Ba}$						
R-HF	2.979	125.7	3.131	138.8	3.322	105.4
R-MP2	2.711	319.0	2.848	292.0	2.998	163.3
R-CCSD	2.811	263.2	2.951	238.9	3.126	136.1
R-CCSD(T)	2.789	286.2	2.930	255.7	3.102	142.9
NR-HF	3.490	62.7	3.595	54.7	3.856	70.7
NR-MP2	3.055	169.1	3.146	138.4	3.325	127.4

[a] Results for  $\text{AuHg}^+$  are taken from ref. [5].

cationic dimers fulfill the formal criterion for CSI since they consist of two interacting closed-shell fragments, the  $d^{10}$  gold cation and a closed-shell atom. However, significant charge transfer from the neutral atom to the gold cation at the equilibrium distance and low-lying alternative dissociation channels indicate a contribution from open-shell configurations to the bonding. Even though the degree of covalency in  $\text{RgAu}^+$  and related species remains subject to discussion,<sup>[7]</sup> these compounds are clearly different from the aforementioned examples. Their highest occupied molecular orbitals

[\*] Prof. Dr. P. Schwerdtfeger, Dr. R. Wesendrup  
Department of Chemistry  
University of Auckland  
Private Bag 92019, Auckland (New Zealand)  
Fax: (+64) 9-3737422  
E-mail: schwerd@ccu1.auckland.ac.nz

[\*\*] This work was supported by the Auckland University Research Committee, the Deutsche Forschungsgemeinschaft (DFG), and the Marsden Fund managed by the Royal Society of New Zealand. We are grateful to Prof. W. H. E. Schwarz (Siegen) for his critical and most valuable comments.